

ARMY RESEARCH LABORATORY



## **Interactions of Organic Surfactants With Oxide Nanoparticles Grown in Aqueous Environments**

by Jennifer Synowczynski

ARL-TR-4047

February 2007

## **NOTICES**

### **Disclaimers**

The findings in this report are not to be construed as an official Department of the Army position unless so designated by other authorized documents.

Citation of manufacturer's or trade names does not constitute an official endorsement or approval of the use thereof.

Destroy this report when it is no longer needed. Do not return it to the originator.

# **Army Research Laboratory**

Aberdeen Proving Ground, MD 21005-5069

---

**ARL-TR-4047**

**February 2007**

---

## **Interactions of Organic Surfactants With Oxide Nanoparticles Grown in Aqueous Environments**

**Jennifer Synowczynski  
Weapons and Materials Research Directorate, ARL**

<b>REPORT DOCUMENTATION PAGE</b>				<i>Form Approved OMB No. 0704-0188</i>	
<p>Public reporting burden for this collection of information is estimated to average 1 hour per response, including the time for reviewing instructions, searching existing data sources, gathering and maintaining the data needed, and completing and reviewing the collection information. Send comments regarding this burden estimate or any other aspect of this collection of information, including suggestions for reducing the burden, to Department of Defense, Washington Headquarters Services, Directorate for Information Operations and Reports (0704-0188), 1215 Jefferson Davis Highway, Suite 1204, Arlington, VA 22202-4302. Respondents should be aware that notwithstanding any other provision of law, no person shall be subject to any penalty for failing to comply with a collection of information if it does not display a currently valid OMB control number.</p> <p><b>PLEASE DO NOT RETURN YOUR FORM TO THE ABOVE ADDRESS.</b></p>					
<b>1. REPORT DATE (DD-MM-YYYY)</b> February 2007		<b>2. REPORT TYPE</b> Final		<b>3. DATES COVERED (From - To)</b> September 2005–August 2006	
<b>4. TITLE AND SUBTITLE</b>  Interactions of Organic Surfactants With Oxide Nanoparticles Grown in Aqueous Environments		<b>5a. CONTRACT NUMBER</b>			
		<b>5b. GRANT NUMBER</b>			
		<b>5c. PROGRAM ELEMENT NUMBER</b>			
<b>6. AUTHOR(S)</b>  Jennifer Synowczynski		<b>5d. PROJECT NUMBER</b> AH84			
		<b>5e. TASK NUMBER</b>			
		<b>5f. WORK UNIT NUMBER</b>			
<b>7. PERFORMING ORGANIZATION NAME(S) AND ADDRESS(ES)</b>  U.S. Army Research Laboratory ATTN: AMSRD-ARL-WM-MA Aberdeen Proving Ground, MD 21005-5069		<b>8. PERFORMING ORGANIZATION REPORT NUMBER</b>  ARL-TR-4047			
<b>9. SPONSORING/MONITORING AGENCY NAME(S) AND ADDRESS(ES)</b>		<b>10. SPONSOR/MONITOR'S ACRONYM(S)</b>			
		<b>11. SPONSOR/MONITOR'S REPORT NUMBER(S)</b>			
<b>12. DISTRIBUTION/AVAILABILITY STATEMENT</b>  Approved for public release; distribution is unlimited.					
<b>13. SUPPLEMENTARY NOTES</b>					
<b>14. ABSTRACT</b>  The goal of this report is to provide a fundamental understanding of how organic surfactants with different functional endgroups and branching structures affect the surface chemistry, organization, and growth of oxide nanoparticles (e.g., TiO <sub>2</sub> , ZnO) in aqueous solutions. It is generally known that particles grow from solution into shapes that minimize their surface free energy $\gamma$ . The surface free energy is a complex function of the surface area, crystal anisotropy and defect structure, degree of coordination unsaturation, surface polarity, reconstruction barriers, and stoichiometry gradients. In solution, the situation is further complicated by changes in pH as well as interactions with ions and surfactants. Whether an ion or surfactant adsorbs to a specific facet depends on the competition between electrostatic and hydrophobic forces as well as their ability to form chemical complexes with the surface. By engineering these surface interactions, one can either promote or prevent particle growth along specific crystallographic planes. Using this approach, researchers have succeeded in precipitating particles with atypical shapes such as nanotubes, rods, cubes, and monodispersed spheres. A firm understanding of the relationship between solution chemistry and the complexes that form at the aqueous/TiO <sub>2</sub> surface will greatly enhance our ability to control the morphology of TiO <sub>2</sub> nanoparticles and assemble these particles into more complicated structures. This work is critical to demonstrating many devices that rely on quantum confinement effects, including photonic bandgap devices and self-cleaning photocatalytically active surfaces.					
<b>15. SUBJECT TERMS</b>  titania, nanoparticle, surfactant					
<b>16. SECURITY CLASSIFICATION OF:</b>		<b>17. LIMITATION OF ABSTRACT</b>	<b>18. NUMBER OF PAGES</b>	<b>19a. NAME OF RESPONSIBLE PERSON</b> Jennifer Synowczynski	
<b>a. REPORT</b> UNCLASSIFIED	<b>b. ABSTRACT</b> UNCLASSIFIED	<b>c. THIS PAGE</b> UNCLASSIFIED	UL	28	<b>19b. TELEPHONE NUMBER</b> (Include area code) 410-306-0750

---

## Contents

---

<b>List of Figures</b>	<b>v</b>
<b>List of Tables</b>	<b>v</b>
<b>1. Introduction</b>	<b>1</b>
<b>2. Bulk Crystalline Structure</b>	<b>1</b>
<b>3. Driving Forces for Adsorption at TiO<sub>2</sub> Surfaces</b>	<b>2</b>
3.1 Effect of Crystal Structure on the Degree of Coordination Unsaturation .....	3
3.2 Surface Polarity .....	3
3.3 Defect Structure.....	3
<b>4. What Happens to Oxide Surfaces in Aqueous Solutions?</b>	<b>5</b>
4.1 Hydroxylation of the Particle Surface .....	5
4.2 Electric Double Layer .....	6
<b>5. Factors to Consider in the Design of Surfactants</b>	<b>6</b>
5.1 Gibbs Free Energy of Adsorption .....	6
5.2 Acid/Base Behavior of Functional Groups .....	7
5.2.1 Polarizability .....	7
5.2.2 The Role of Hydrogen Bonding .....	7
5.2.3 Steric Forces .....	8
<b>6. Preliminary Results From Surfactant Templated Hydrothermal Reactions</b>	<b>9</b>
<b>7. Results</b>	<b>10</b>
<b>8. Future Work</b>	<b>10</b>
8.1 Wet Chemical Adsorption Isotherms .....	11
8.2 Infrared Spectroscopy.....	15
8.3 X-ray Absorption Fine Structure .....	16

**9. References** **18**

**Distribution List** **20**

---

## List of Figures

---

Figure 1. Bulk crystal structure of anatase and rutile with bond angles and lengths (3).....	2
Figure 2. Ball and stick model of rutile crystal structure showing charge-neutral cleavage along the (110) surface.....	4
Figure 3. Ball and stick model of rutile crystal structure showing charge-neutral cleavage along the (100) surface.....	4
Figure 4. Ball and stick model of rutile crystal structure showing charge-neutral cleavage along the (001) surface.....	4
Figure 5. Structural model for the adsorption of water to $\text{TiO}_2$ surfaces.....	5
Figure 6. TEM pictures of $\text{TiO}_2$ particles precipitated from hydrothermal solutions under different acidic conditions.....	11
Figure 7. TEM pictures of $\text{TiO}_2$ particles precipitated from hydrothermal solutions in the presence of different surfactants.....	12
Figure 8. TEM pictures of $\text{TiO}_2$ particles precipitated from different solvents.....	13
Figure 9. TEM Pictures of $\text{TiO}_2$ rods precipitated under different acidic conditions from hydrothermal solutions containing ammonium phosphate. ....	13
Figure 10. Sorption of Co(II) on showing $\alpha\text{SiO}_2$ , rutile $\text{TiO}_2$ , $\text{Fe}_2\text{O}_3$ , $\text{Al}_2\text{O}_3$ (a) pH dependence and (b) relative influence of $\text{pH}_{\text{zpc}}$ .....	14

---

## List of Tables

---

Table 1. Ionization potentials of organic compounds with different functional groups.....	8
Table 2. Force constants and equilibrium bond distances for many common elements.....	9
Table 3. Morphology results for different surfactant additives. ....	9
Table 4. Absorption bands for different Ti coordinations and hydroxyl groups probed with $\text{CO}$ , $\text{NH}_2$ , and $\text{SO}_2$ .....	16

INTENTIONALLY LEFT BLANK.

---

## 1. Introduction

---

Much of what is known about the surface chemistry of  $\text{TiO}_2$  surfaces comes from modeling and from ultrahigh vacuum (UHV) studies of carefully prepared single crystalline surfaces. Sections 2 and 3 of this report highlight the knowledge gained from these studies. They are critical to our understanding of the natural tendencies and anisotropies inherent in  $\text{TiO}_2$  crystals. However, the situation in aqueous solutions is further complicated by the adsorption of hydroxyls, ions, and surfactants. Molecular adsorption disrupts the balance between the electrostatic, hydrophobic, and steric forces, and it creates kinetic barriers to particle growth. These effects are the focus of this research and will be further discussed in section 4. Section 5 reviews what is known about the coordinating tendencies of different organic molecules as a function of their molecular chain length, branching structure, and functional group. Section 6 describes some preliminary results from hydrothermal reactions that suggest the preferential adsorption of organic surfactants for specific crystalline facets. Section 7 describes the questions that arise from the preliminary results and recommends future work.

---

## 2. Bulk Crystalline Structure

---

The most important predictor of the surface chemistry under UHV conditions is the bulk crystalline structure. It influences the preferred crystal orientation, defect structure, surface stability, and chemical reactivity. There are seven known polymorphs of titania, only four of which (rutile, brookite, anatase, and  $\text{TiO}_2$  B [see figure 1]) occur in nature. The anatase and rutile phases are the focuses of this investigation. Their bases consist of Ti octahedrally coordinated to oxygen. The right side of figure 1 shows the octahedra stacked so that each oxygen has three-fold coordination. For particle sizes that are less than 11 nm, the thermodynamically favored phase is anatase (tetragonal  $D_{4h}^{19} - I4_1 / amd$ ,  $a = b = 3.782 \text{ \AA}$ ,  $c = 9.502 \text{ \AA}$ ). As the particle grows from 11 to 35 nm, it transforms into brookite (rhombohedral,  $D_{2h}^{15} - Pbca$ ,  $a = 5.436 \text{ \AA}$ ,  $b = 9.166 \text{ \AA}$ ,  $c = 5.135 \text{ \AA}$ ). Particle sizes greater than 35 nm typically form the rutile phase (tetragonal  $D_{4h}^{14} - P4_2 / mnm$ ,  $a = b = 4.584 \text{ \AA}$ ,  $c = 2.953 \text{ \AA}$ ). Under extremely high pressures,  $\text{TiO}_2$  can also form an orthorhombic dipyramidal cotunnite phase (1).

The particle sizes at which these phase transformations occur can be artificially engineered through surfactant and solvent interactions during crystallization. There is some discussion in the literature as to which phase is promoted during hydrothermal treatment. In one case, it was found that acidic conditions resulted in the formation of anatase, rutile, and brookite, whereas only the anatase phase precipitated under basic conditions or in the presence of chloride ions (2).

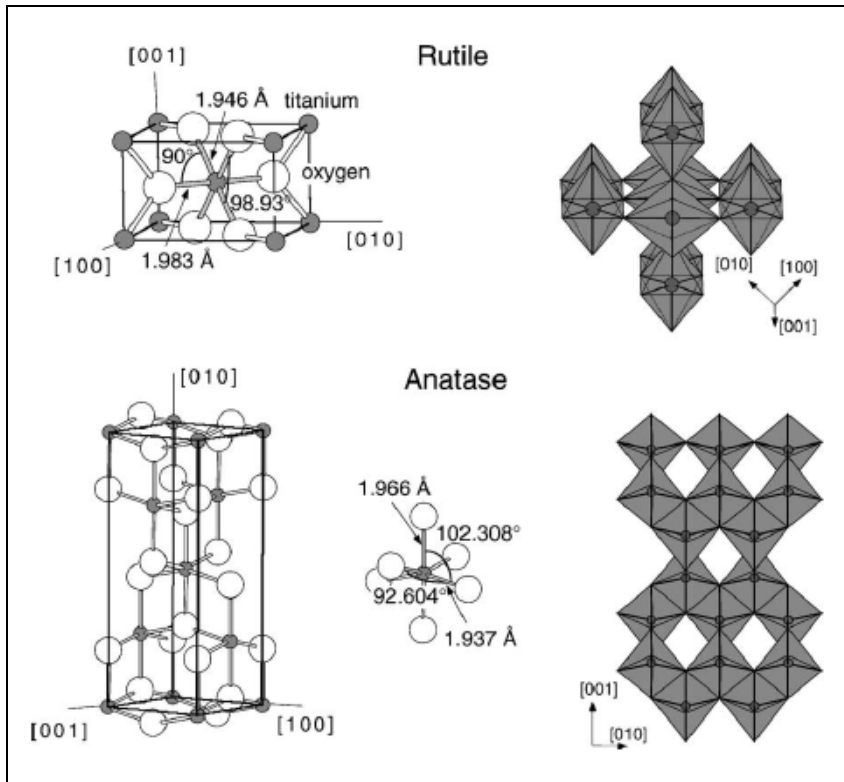


Figure 1. Bulk crystal structure of anatase and rutile with bond angles and lengths (3).

When the precursor and solvent were changed from titanium tetrachloride and water to titanium oxychloride and water/2-propanol, the precipitated phase was rutile (4). However, adding sulfate ions promoted the formation of anatase. As will be discussed in the later sections of the report, the solvent and precursor chemistry affects the complexes that form at the  $\text{TiO}_2$  surface during crystallization. These studies highlight the importance of understanding the effects of surface chemistry and interactions on the kinetics and thermodynamics of the crystallization processes.

### 3. Driving Forces for Adsorption at $\text{TiO}_2$ Surfaces

All thermodynamically stable processes evolve in a manner which minimizes the free energy of the system. For nanoparticles, the energetics of the system is dominated by the energy of the particle surface. There are two driving forces for molecular adsorption. They are the desire to fulfill the atomic coordination of the surface atoms and the desire to maintain the electrical neutrality of the surface. The effect of crystal orientation and defect structure on these forces is described next.

### 3.1 Effect of Crystal Structure on the Degree of Coordination Unsaturation

The minimum energy configuration for surface atoms is that which most closely mimics the coordination environment of the bulk atoms. However, due to the truncation of the crystal, surface atoms are not fully coordinated. The degree of coordination unsaturation depends on which crystalline facet terminates the surface. This can be determined for single crystal surfaces under high vacuum conditions using atomic force microscopy, low energy electron diffraction, or reflection high-energy electron diffraction. For the rutile (110) facet, half of the Ti atoms retain their six-fold coordination, while the other half remains in five-fold coordination. The stability decreases for the (100) and (001) facets as the coordination for the Ti atoms falls to five-fold and four-fold, respectively. For anatase, the (101) surface is the most stable with a surface free energy lower than even the rutile (110) (5). As the degree of coordination unsaturation increases, the driving force for chemical and physical adsorption also increases. If there are no adsorption species available, surface atoms will relax into configurations that maximize their coordination and stabilize the electrostatic interactions (6).

### 3.2 Surface Polarity

A second consequence of coordination unsaturation is the creation of dangling bonds with excess charge. In order for a surface to be stable, these dangling bonds must produce no net dipole moment. This can occur if the individual planes are neutral (i.e., there are equal numbers of atoms with opposite charges on the same plane) or if alternately charged planes are symmetrically stacked. The latter is the case for the nonpolar rutile (110) surface (7). The area defined by the dashed lines A and B in figure 2 represents an electrically neutral repeat unit for the rutile (110) surface. It consists of three layers: two negatively charged layers containing only O<sup>-2</sup> atoms surrounding a positively charged layer that contains an equal number of Ti<sup>+4</sup> and O<sup>-2</sup> atoms. A similar analysis for rutile (100) and (001) predicts electrostatically stable cleavage along the dashed line in figures 3b and 4, respectively (8). Although the cleavage is electrostatically stable for the (001) termination, it is not thermodynamically stable because of the low coordination of the Ti (four-fold) and O atoms (two-fold). The cleavage planes drawn in figures 2–4 represent theoretical calculations of electrostatically stable surfaces in UHV environments. Additional planes can also be electrostatically stabilized by the adsorption of ions from solution.

### 3.3 Defect Structure

The equilibrium configurations adopted by surface atoms can also be locally disrupted by the presence of surface defects including oxygen vacancies, monatomic steps, kinks, and dislocations. As an example, consider the importance of defects in the adsorption of water under UHV conditions. Most UHV studies agree that water can dissociate and adsorb molecularly on perfect rutile (100) surfaces (9) even in the absence of defects. However, experimental evidence suggests that oxygen vacancies are necessary in order to dissociate water on the rutile (110) facets.

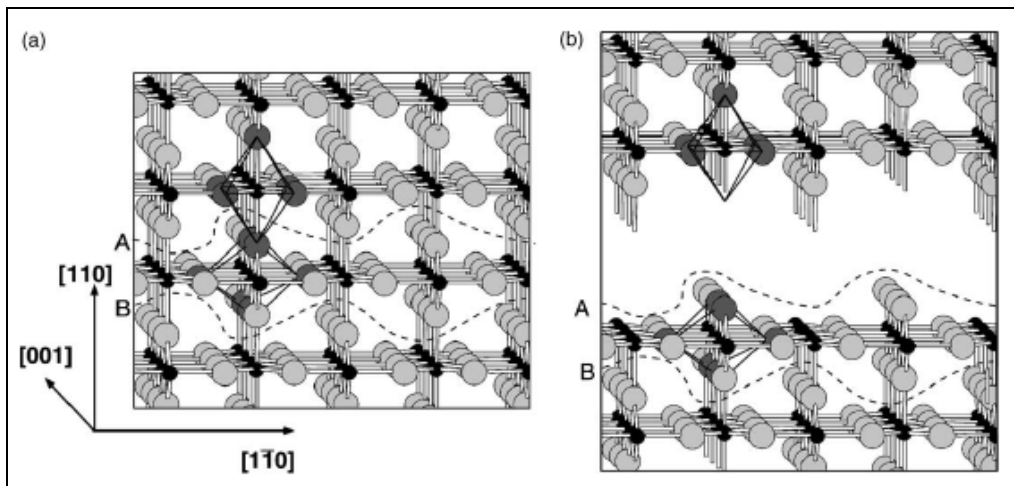


Figure 2. Ball and stick model of rutile crystal structure showing charge-neutral cleavage along the (110) surface.

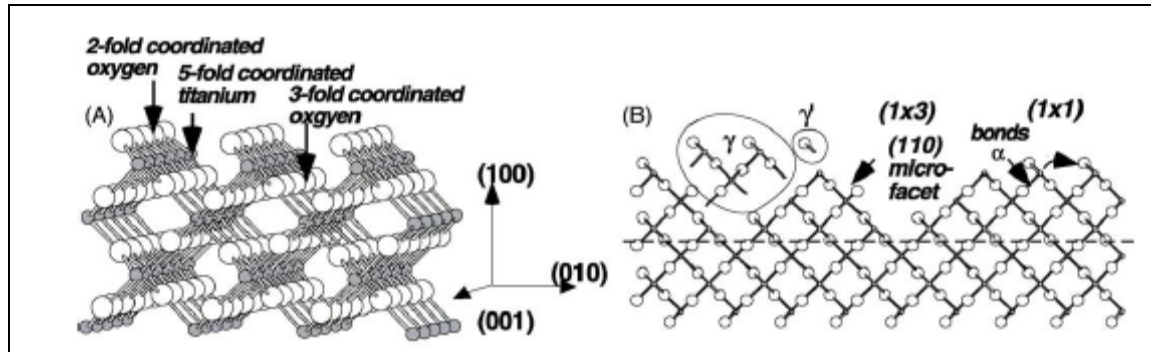


Figure 3. Ball and stick model of rutile crystal structure showing charge-neutral cleavage along the (100) surface.

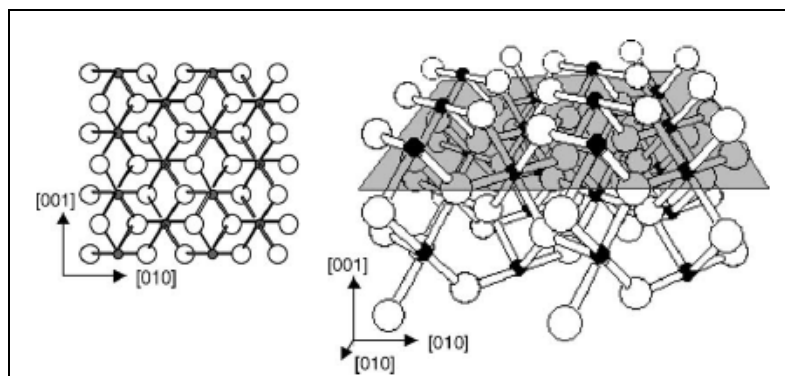


Figure 4. Ball and stick model of rutile crystal structure showing charge-neutral cleavage along the (001) surface.

This may be due to hydrogen bonding (see figure 5). Along a rutile (100) faceted crystal, the distance between the oxygen atoms in the adsorbed water and the two-fold oxygen atoms in the  $\text{TiO}_2$  crystal allows for weak hydrogen bonding. However, for rutile (110) oriented crystals, this distance is at least 3.2 Å, making it impossible for water to form hydrogen bonds except at oxygen vacancies, which allow the water to come closer to the surface.

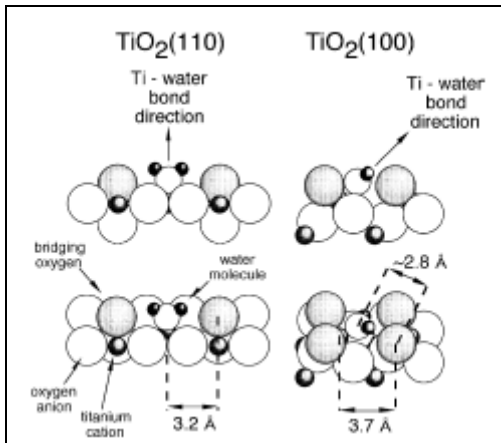


Figure 5. Structural model for the adsorption of water to  $\text{TiO}_2$  surfaces.

Defects are also important initiation sites for nucleation and growth phenomenon. According to Burton-Cabrera-Frank theory, particle growth and dissolution occurs primarily at monatomic steps and kinks created by the surface termination of screw dislocations. These defects have crystallographically preferred growth directions which can be engineered through the adsorption of surfactants (10). Phosphates and phosphonates are especially good at stabilizing defects against dissolution (11).

---

## 4. What Happens to Oxide Surfaces in Aqueous Solutions?

---

### 4.1 Hydroxylation of the Particle Surface

$\text{TiO}_2$  surfaces in contact with aqueous solutions quickly hydrolyze to fulfill their atomic coordination. The water is ordered into two layers, an inner sphere of directly adsorbed water surrounded by an outer sphere of water that is loosely bound by hydrogen bonding. Theoretical studies (12) suggest that structure of water in the inner layer is similar to ice (i.e., the oxygen atoms form puckered hexagons linked by hydrogen bonds). In order to form a complex with the surface, molecules must first form complexes with the outer sphere and then displace the inner sphere water with complexing ligands. The magnitude of the kinetic barrier this poses is a function of the thickness of the hydrogen bonded layer and the strength of the inner sphere

aqueous complexes. As discussed in the previous section, this can be affected by the crystal orientation and defect structure.

## 4.2 Electric Double Layer

When the  $\text{TiO}_2$  surface is immersed in an aqueous environment, it also develops a surface charge because of surface protonation-deprotonation reactions and the specific adsorption of ions from solutions. The surface charge generates an electrostatic force that attracts ions with opposite charge and repels like-charged ions. This tightly bonded inner layer is surrounded by an additional layer of ions that are diffusely bonded to the inner layer by coulombic and hydrogen bonding forces. The two-layer complex is known as an electric double layer. The thickness of the electric double layer is a function of the pH and ionic strength of the solution. The pH at which the surface has a zero charge is called the isoelectric point. The isoelectric point for  $\text{TiO}_2$  is 5.9. Below  $\text{pH} = 5.9$ , the surface has a positive charge. Above 5.9, it is negatively charged. The ability of a surface to neutralize its charge through adsorption depends on the polarity of the surface, the adsorbate, and the solvent. Polar surfaces adsorb polar adsorbates strongly and nonpolar adsorbates weakly, whereas nonpolar surfaces strongly attract nonpolar adsorbates. As the polarity of the solvent increases, adsorbates are more easily ionized. However, the electrostatic field strengths drop off more rapidly. In addition, as the solvent polarity increases, the solvent competes for adsorption to the surface making it difficult to attract polar adsorbates.

---

## 5. Factors to Consider in the Design of Surfactants

---

There are many factors to consider when designing effective surfactants. If the goal is to prevent colloidal particles from agglomerating, the surfactant is designed to enhance its electrosteric stabilization properties. These surfactants have polar headgroups to bind to the acid/base sites of the particle surface and long lyophilic tails that extend into the solution and sterically hinder particle agglomeration. Surfactant design is more complicated if the goal is to control the morphology of particles growing from solution. In order to grow  $\text{TiO}_2$  nanorods, a consistent asymmetry in the dissolution and growth conditions must be created. This can be accomplished by tailoring the affinity of the surfactant for specific crystallographic planes. The factors that affect how a surfactant binds to the surface include its shape, the polarity and ionizability of its functional group, and the location of the functional group relative to other parts of the molecule. These effects are described in further detail in the following sections.

### 5.1 Gibbs Free Energy of Adsorption

Surfactants will bind to the surface in the conformation which minimizes their Gibbs free energy. Some molecules form strong inner sphere complexes with the surface. Others can only form loosely bonded outer sphere complexes because of interference from other parts of the molecule.

The total free energy of adsorption  $\Delta G_{ads}$  can be expressed as the sum of the following free energy contributions:

$$\Delta G_{ads} = \Delta G_{elec} + \Delta G_{chem} + \Delta G_{c-c} + \Delta G_{c-s} + \Delta G_{H-bonding} + \Delta G_{vdw}, \quad (1)$$

where  $\Delta G_{elec} \sim 10$  kJ/mol is the electrostatic interaction term,  $\Delta G_{chem} > 25$  kJ/mol is due to the covalent bonding,  $\Delta G_{c-c} \sim 1$  kJ/mol/chain segment is the lateral chain-chain interaction,  $\Delta G_{c-s} \sim 1$  kJ/mol/chain segment is the interaction between hydrophobic chains and hydrophobic surface sites,  $\Delta G_{H-bonding} \sim 10$  kJ/mol is the hydrogen bonding interaction term, and  $\Delta G_{vdw} \sim 0.1$  kJ/mol is the term due to van der Waals forces. The goal in surfactant design is to tailor the distribution of functional groups to promote hydrogen bonding and electrostatic attraction to the particle surface.

## 5.2 Acid/Base Behavior of Functional Groups

As described next, the acid/base behavior of a particular functional group depends on the polarizability of the bonding, its ability to form hydrogen bonds with the surface and solvent, and the steric environment surrounding the group.

### 5.2.1 Polarizability

The ionization potential is a measure of the amount of energy required to remove an electron from the molecule. The highest ionization energies are for molecules that have a symmetrical charge distribution, such as methane and ethane. As the electronegativity difference between atoms increases, the charge distribution becomes more asymmetrical, and the ionization potential decreases. Nonbonding electrons, such as those on N and O, and the  $\pi$  bonding electrons of alkenes and aromatic molecules are held more loosely than electrons in C-C and C-H  $\sigma$  bonds. Alkyl groups have electron pushing properties. Therefore, adding alkyl groups tends to increase the charge concentration on more highly electronegative elements such as O, N, and F. This is directly reflected by their ionization potentials listed in table 1.

In general, carboxyl, hydroxyl, amine, and ester groups are highly polarizable and make good anchors to particle surfaces.

### 5.2.2 The Role of Hydrogen Bonding

The expected acid/base behavior of functional groups can be modified by hydrogen bonding within the surfactant and with the solvent. From simple structure calculations, you would expect the basicity of the molecule to increase as the hydrogen atoms surrounding the cation are replaced by methyl groups, which have electron pushing tendencies. Although this is true in gas phase reactions, exactly the opposite is true for aqueous reactions. This is because the solvent stabilizes the cation through hydrogen bonding interactions. As the hydrogen groups on the cation are replaced by methyl groups, the number of hydrogen bonding sites is reduced. This explains why the basicity of trimethylamine in water is only slightly higher than ammonia.

Table 1. Ionization potentials of organic compounds with different functional groups.

Chemical Formula	Family	Ionization Potential (eV)
CH <sub>4</sub>	Alkane	12.7
CH <sub>3</sub> CH <sub>3</sub>	Alkane	11.5
CH≡CH	Alkyne	11.4
CH <sub>3</sub> OH	Alcohol	10.8
CH <sub>2</sub> =CH <sub>2</sub>	Alkene	10.5
CH <sub>3</sub> (C=O)OH	Carboxylic acid	10.37
CH <sub>3</sub> (C=O)OCH <sub>3</sub>	Ester	10.27
CH <sub>3</sub> (C=O)H	Aldehyde	10.21
NH <sub>3</sub>	Ammonia	10.2
CH <sub>3</sub> OCH <sub>3</sub>	Ether	9.98
CH <sub>3</sub> (C=O)NH <sub>3</sub>	Amide	9.77
CH <sub>3</sub> (C=O)CH <sub>3</sub>	Ketone	9.69
C <sub>6</sub> H <sub>6</sub>	Arene	9.2
CH <sub>3</sub> NH <sub>2</sub>	Amine	8.97
C <sub>2</sub> H <sub>5</sub> NH <sub>2</sub>	Amine	8.86
(CH <sub>3</sub> ) <sub>2</sub> NH	2° Amine	8.24

### 5.2.3 Steric Forces

The adsorption behavior of organic molecules is also influenced by steric forces. There are two major steric forces to consider: steric strain due to the distortion of the bonding structure within the molecule and steric interference caused by the nonbonding groups along the molecule.

Steric strain is generated during the distortion of the bonding structure from thermodynamically preferred bond lengths and bond angles. The strain energy is an important measure of how well a ligand is sterically suited to complex to the TiO<sub>2</sub> surface. There are two contributions to the strain energy: bond length distortion and angular distortion. They can be directly calculated from Hooke's law:

$$U_B = \frac{1}{2} K_B (r - r^o)^2, \quad (2)$$

where  $U_B$  is the strain energy due to bond length distortion,  $K_B$  is the force constant for restoring the bond to its ideal length  $r^o$ , and  $r$  is the length to which the bond has been distorted. The force constant ( $K_B$ ) is proportional to the strength of the covalent bond. It is smallest for H-H and O-H bonds, followed by N-H and C-H bonding (see table 2).

The bond angle distortion can also be calculated using Hooke's law:

$$U_\theta = \frac{1}{2} K_\theta (\theta - \theta^o)^2, \quad (3)$$

where  $U_\theta$  is the strain energy produced during bond angle distortion,  $K_\theta$  is the force constant for restoring the bond angle its ideal value  $\theta^o$ , and  $\theta$  is the observed bond angle.

Table 2. Force constants and equilibrium bond distances for many common elements.

Atom No. 1	Atom No. 2	Bond Length (Å)	Force Constant
H	H	0.738	4.661
H	O	0.96	5.794
H	N	1.01	6.057
H	C	1.09	6.217
H	P	1.41	7.257
C	O	1.44	7.347
C	N	1.47	7.504
N	O	1.42	7.526
C	C	1.526	7.643
O	P	1.64	7.957
C	P	1.83	8.237
C	Cl	1.8	8.241
N	Cl	1.75	8.266

Steric interference occurs when the functional group is surrounded by nonbonding groups (i.e., methyl groups) that prevent interaction with the surface. P-R<sub>3</sub> and S-R<sub>2</sub> functional groups typically have lower steric hindrances because the P-C and S-C bonds are longer than N-C and O-C bonds. This causes the methyl groups to be held further away from the proton. In general, steric interference increases as chain length and branching increases.

## 6. Preliminary Results From Surfactant Templated Hydrothermal Reactions

A preliminary investigation was conducted in order to determine the effect of surfactants (listed in table 3) on the morphological evolution of hydrothermally precipitated TiO<sub>2</sub> nanopowders using the synthesis method described in the following section.

Table 3. Morphology results for different surfactant additives.

Additive	Morphology	~Size (nm)	~Aspect Ratio
No additive	Equiaxed polyhedra	50–100	1
Triethanolamine	Elongated polyhedra	50–100	2
Cyclohexylamine	Bullet-like w/snow	50–100	2
Triethylamine	Elongated polyhedra	50–100	2
Ethanolamine	Bullet-like w/snow	100–200	1
Ammonium phosphate	Bullet-like	50–100	5
Ammonium chloride	Equiaxed polyhedra	10–25	1
n-butylamine	Equiaxed polyhedra	50–100	1
Ethylene glycol	Equiaxed polyhedra	10–25	1
Di-isopropylamine	Equiaxed polyhedra	25–100	1

## Synthesis Method

First, 0.1 M  $\text{TiCl}_4$  was added to high-performance liquid chromatography grade deionized water and neutralized with 0.4 M NaOH (J. T. Baker, Sweden, 95% pure) to form amorphous titania  $\text{TiO}_2 \cdot n\text{H}_2\text{O}$ . Since  $\text{TiCl}_4$  reacts with water exothermically to generate orthotitanic acid  $[\text{Ti}(\text{OH})_4]$ , extra care was taken during handling. The amorphous titania was then washed and centrifuged (Avanti J25, Beckman-Coulter) three times at 5000 RPM for 20 min to remove any chlorine ions. Next, the surfactants and pH adjusters ( $\text{NH}_4\text{OH}$  or HCl) were added. After 15 hr of mixing, the reagents were charged into 110-mL stainless steel Teflon<sup>\*</sup>-lined autoclaves (Parr Instruments, Moline, IL) that were heated by mantles (Glas-Col, Terre Haute, IN) to 160 °C for 6 hr. The products were then cooled to room temperature and vacuum-filtered through 0.22- $\mu\text{m}$  Teflon-coated filter paper (Millipore Corp., Bedford, MA). Powders were again washed and centrifuged three times prior to transmission electron microscopy (TEM) analysis.

---

## 7. Results

---

From the TEM pictures shown in figures 6–9 and the morphology results in table 3, the following trends are clear: (1) as the pH of the solution increases, the particle shape becomes more elongated and (2) primary amines and ammonium phosphate promote the formation of  $\text{TiO}_2$  rods. Since nonselective adsorption of organic surfactants creates a kinetic barrier to the deposition of new oxide layers, one would expect very small equiaxed particles to form. Similarly, if the surfactant selectively adsorbs to specific crystallographic planes, there is a kinetic barrier to the vertical growth rate of that plane. This would create particles with elongated rod-like morphologies. This logic suggests that triethanolamine, tributylamine, n-butylamine, ammonium chloride, di-isopropylamine, and ethylene glycol bind nonselectively, whereas ethanolamine, cyclohexylamine, and ammonium phosphate bind selectively to the surface. However, it is not possible to say for sure what is happening without further spectroscopic investigations.

---

## 8. Future Work

---

In order to understand how the morphology of  $\text{TiO}_2$  particles evolves as a function of surface and solution chemistry, it is important to have a detailed picture of the following phenomena: (1) chemical speciation, (2) aqueous complexes formed around particle surface, surfactants, and Ti precursors, (3) thickness of the electric double layer and distribution of ions near the surface as a function of pH, ionic strength, and surfactants, (4) conformation and binding affinities of the organic molecules in solution, (5) adsorption bonding mode (i.e., inner sphere or outer sphere) and geometry.

---

<sup>\*</sup>Teflon is a trademark of E.I. du Pont de Nemours and Company.

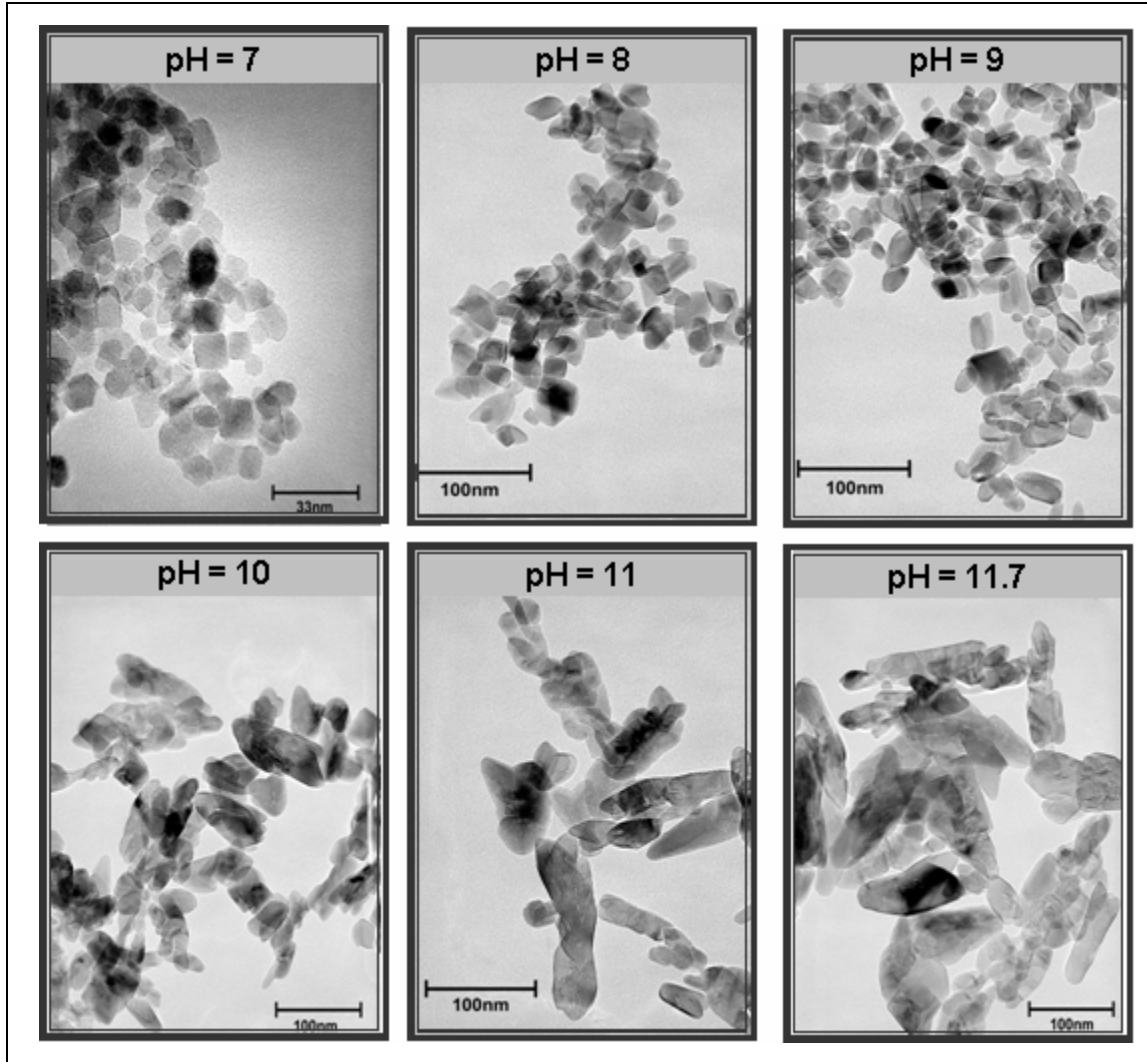


Figure 6. TEM pictures of  $\text{TiO}_2$  particles precipitated from hydrothermal solutions under different acidic conditions.

The effect of surfactant interactions and surface chemistry on the particle morphology can be monitored post-synthesis using TEM. However, there is no single spectroscopic method that can directly measure the changing chemical environment *in situ* without affecting the dynamics of the reaction. However, a description of a combination of spectroscopic methods that can provide useful insight is next.

### 8.1 Wet Chemical Adsorption Isotherms

Adsorption isotherms use spectroscopic methods to measure the amount of adsorbed surfactant at the solid surface versus the equilibrium solution concentration at a given temperature. The initial slope gives an indication of the ease of polymer adsorption. The shape of the isotherm as a function of ionic strength provides information about the adsorption bonding mode. In general, a strong dependence on the ionic strength indicates that the surfactant forms weakly bound outer

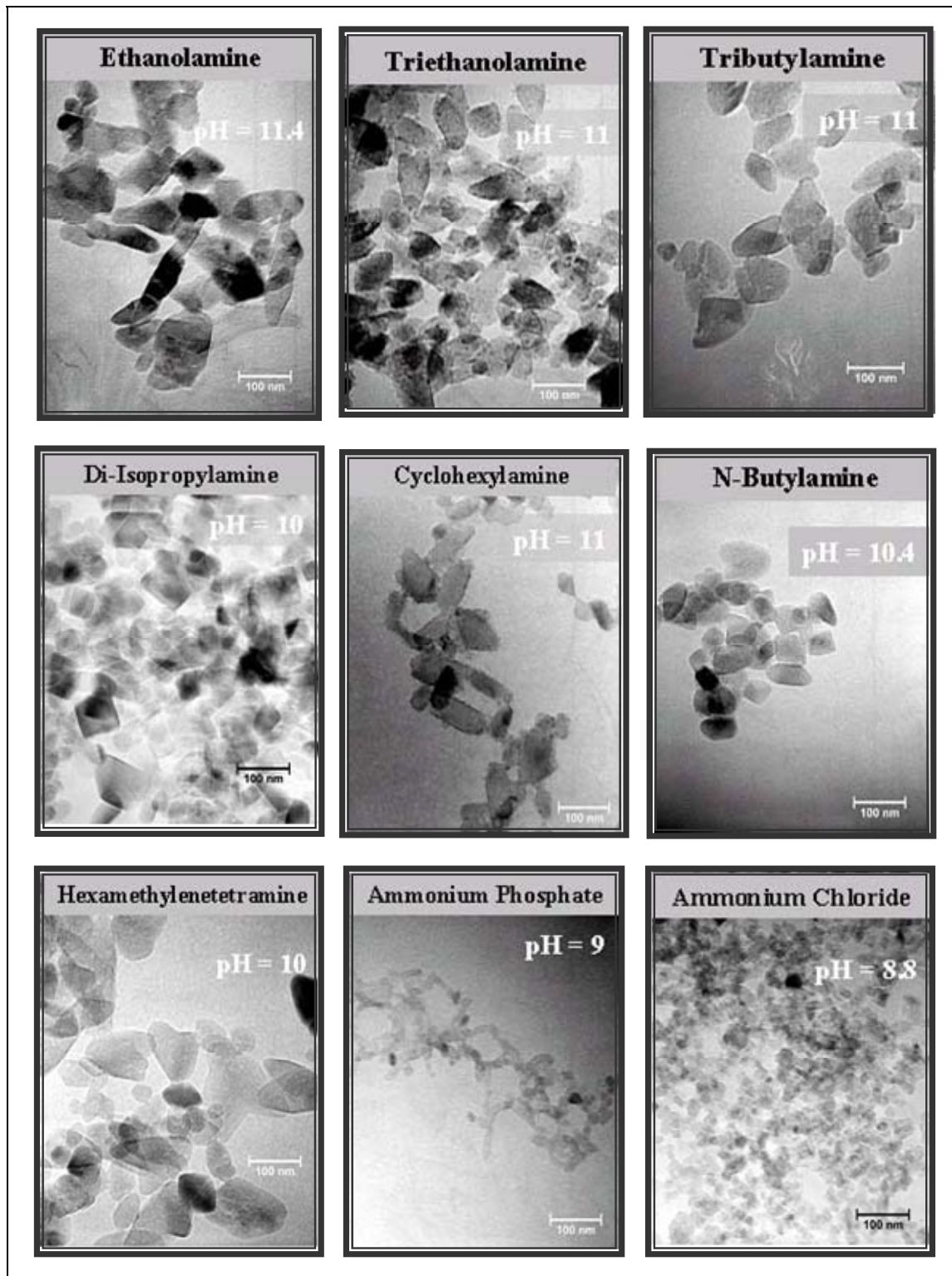


Figure 7. TEM pictures of  $\text{TiO}_2$  particles precipitated from hydrothermal solutions in the presence of different surfactants.

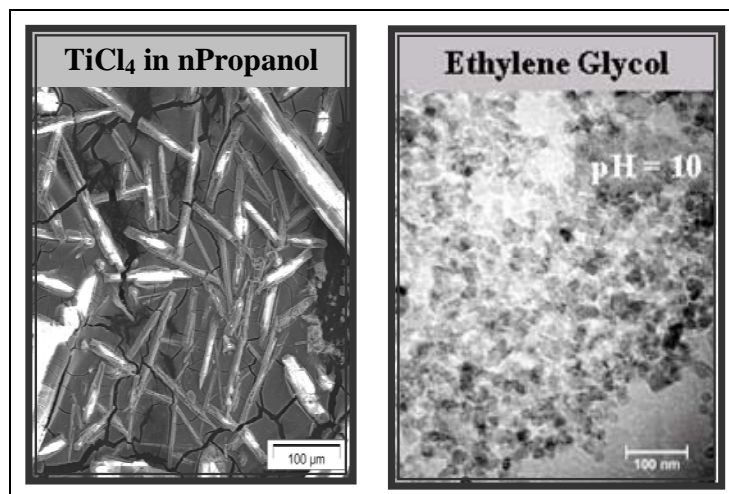


Figure 8. TEM pictures of TiO<sub>2</sub> particles precipitated from different solvents.

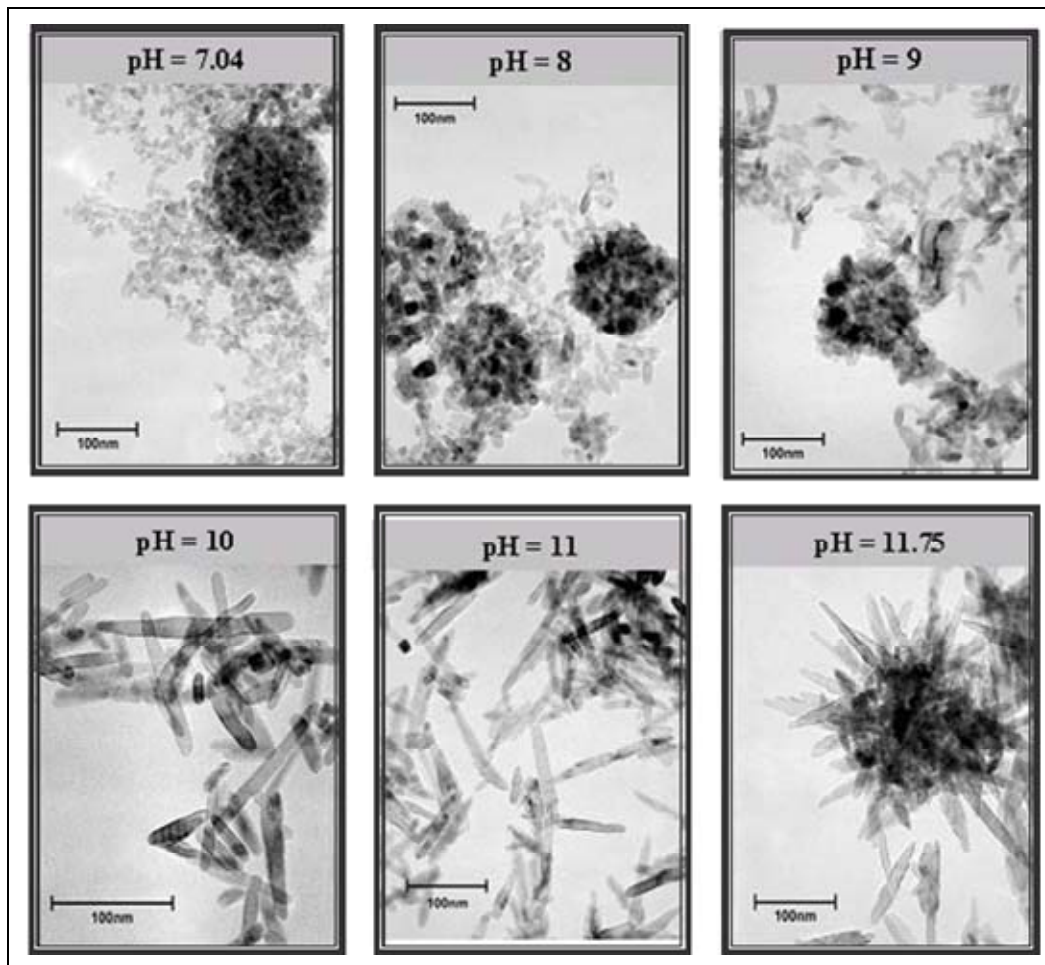


Figure 9. TEM Pictures of TiO<sub>2</sub> rods precipitated under different acidic conditions from hydrothermal solutions containing ammonium phosphate.

sphere complexes whereas no dependence indicates the formation of inner sphere complexes (13). The relative binding strength can be determined from the difference between the  $\text{pH}_{\text{pzc}}$  of the surface and the  $\text{pH}_{\text{ads}}$  (pH at which 50% of the total surfactant is adsorbed). By analyzing the position of the  $\text{pH}_{\text{ads}}$  relative to the  $\text{pH}_{\text{pzc}}$ , it is possible to infer whether the Gibbs free energy of adsorption is dominated by reductions in bond energies, electrostatic attraction, hydrophobic interaction, changes in surface hydration, or protonation/deprotonation reactions. An example of this type of experiment is shown in figure 10 for the adsorption of aqueous Co(II) onto oxide surfaces at different pH (14). The shaded area in the figure represents the range for the  $\text{pH}_{\text{pzc}}$  of the surface ( $\alpha\text{SiO}_2 \sim 2-3$ , rutile  $\text{TiO}_2 \sim 6.9$ ,  $\text{Fe}_2\text{O}_3 \sim 8$ ,  $\text{Al}_2\text{O}_3 \sim 8.5$ ).

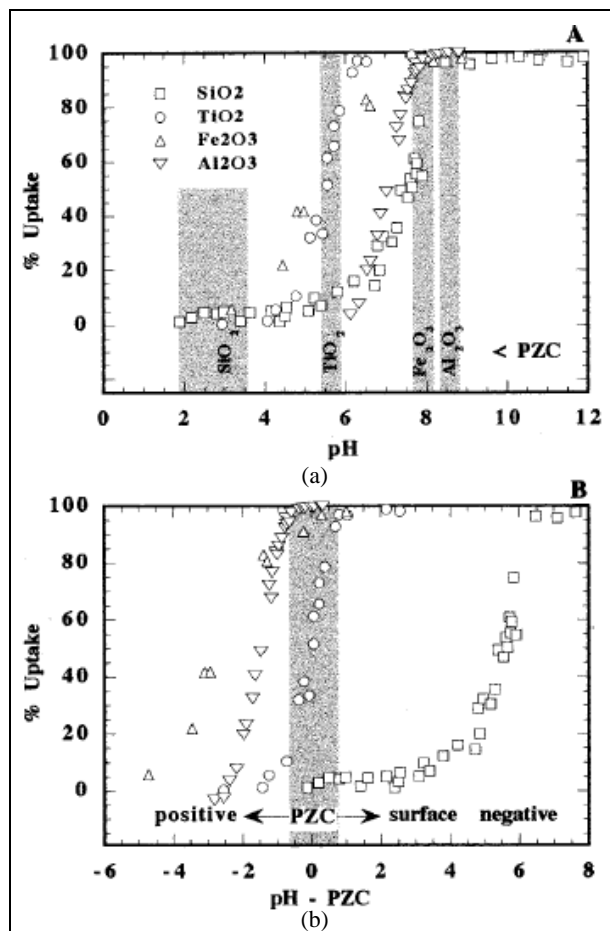


Figure 10. Sorption of Co(II) on showing  $\alpha\text{SiO}_2$ , rutile  $\text{TiO}_2$ ,  $\text{Fe}_2\text{O}_3$ ,  $\text{Al}_2\text{O}_3$  (a) pH dependence and (b) relative influence of  $\text{pH}_{\text{pzc}}$ .

When the adsorption begins near the  $\text{pH}_{\text{pzc}}$  (as is the case for  $\text{TiO}_2$ ), we conclude that electrostatic attraction plays a significant role in the free energy equation. Conversely, when the adsorption is completed below the  $\text{pH}_{\text{pzc}}$  (i.e., under electrostatic repulsion), the free energy equation is dominated by changes due to bonding, hydrophobic interactions, and protonation-

deprotonation reactions. This is the case for  $\text{Fe}_2\text{O}_3$  and  $\text{Al}_2\text{O}_3$  surfaces. For  $\text{SiO}_2$  surface, Co(II) adsorption is delayed until well above the  $\text{pH}_{\text{zpc}}$ . This suggests that one of the variables in the Gibbs free energy equation has a significant positive contribution.

These types of studies will allow us to understand how changing the structure of surfactants affects the relative contributions to the Gibbs free energy equations. It is important to remember, however, that these isotherms are performed on solutions of many precipitating particles. Therefore, they reflect an average over many differently oriented crystallographic surfaces and multiple reactive sites. They cannot provide specific information on the composition or structure of the sorbate, the sorption reactions, or the sites to which the surfactants bind.

## 8.2 Infrared Spectroscopy

Infrared spectroscopy probes the vibrational energy spectrum of the bonding within crystalline materials and organic molecules. Transitions between different vibrational energy states can be induced by the adsorption of infrared radiation with exactly matched energies. However, not all molecular vibrations lead to observable infrared absorptions. In general, a vibration must cause a change in the charge distribution within a molecule to absorb infrared light. The frequencies that are absorbed depend on the atomic masses and force constants:

$$\tilde{\nu} = \frac{1}{2\pi c} \sqrt{\frac{f(m_1 + m_2)}{m_1 + m_2}}, \quad (4)$$

where  $\tilde{\nu}$  is the vibrational frequency,  $f$  is the force constant, and  $c$  is the velocity of light. The force constant is proportional to the strength of the covalent bond. It is typically higher for stretching modes than for bending modes, since it requires more energy to stretch (or compress) a bond than to bend it. The bond dissociation energy is directly proportional to the stretching mode frequency.

Infrared spectroscopy of the interaction between molecular probes and oxide surfaces can provide important information about the acid base behavior of the surface, its defect structure, and nature of the sorbates and hydroxyls as a function of crystal orientation. When the surface is terminated by different facets, the coordination number of surface atoms changes. Decreasing the coordination number of a metal atom at constant valence reduces the interatomic distance and increases the number of valence electrons per bond (i.e., increases the bond multiplicity). Therefore, the strength and frequency of the bond should increase accordingly. Table 4 shows the different types of coordination and oxidation states that can exist for Ti on different exposed surfaces and their absorption frequencies with different molecular probes.

Ideal probe molecules should be sensitive to the strength of the bonding, should be able to distinguish between sorption and protonic (Bronsted) and aprotic (Lewis) acid sites, and should have a size that is comparable to the size of reactants. The most frequently used probe molecules are ammonia, pyridine, aliphatic amines, nitriles, benzenes, and carbon monoxide. The ammonia

Table 4. Absorption bands for different Ti coordinations and hydroxyl groups probed with CO, NH<sub>2</sub>, and SO<sub>2</sub>.

State	Molecule	Bands
Anatase Ti <sup>4+</sup> <sub>cus</sub>	CO	2188, 2208
Anatase Ti <sup>3+</sup> <sub>cus</sub>	CO	2115
Anatase Ti <sup>4+</sup> <sub>5C</sub>	CO	2205
Anatase Ti <sup>4+</sup> <sub>4C</sub>	CO	2190
Anatase OH.....NH <sub>3</sub>	NH <sub>3</sub>	3360
Anatase H <sub>2</sub> NH.....O	NH <sub>3</sub>	3360
Rutile OH.....NH <sub>3</sub>	NH <sub>3</sub>	3310, 1620
Rutile H <sub>2</sub> NH.....O	NH <sub>3</sub>	3310, 1620
	SO <sub>2</sub>	1440, 1330
	SO <sub>2</sub>	1440, 1330
	SO <sub>2</sub>	1440, 1330
	SO <sub>2</sub>	1180

molecule can bond to the oxide surface via three different mechanisms: (1) hydrogen bonding to oxygen from surface oxygen atoms and surface hydroxyls, (2) hydrogen bonding between the nitrogen and a surface hydroxyl, and (3) coordination bond with a surface cation. It can also form NH<sup>4+</sup> ions or completely dissociate and form surface NH<sub>2</sub> and OH groups. The formation of NH<sup>4+</sup> ions during the adsorption of ammonia indicates the presence of Bronsted acid centers, whereas coordinated ammonia indicates Lewis acid sites. However, these methods are not inherently surface specific. Infrared spectra must be corrected for the background adsorption due to the solvent and bulk crystal structure. Background absorption often dominates the relatively weak infrared contribution from the surface. The only way to reduce the background contribution is to reduce the path length through the bulk solution. This can be done using an attenuated total reflection accessory.

### 8.3 X-ray Absorption Fine Structure

X-ray absorption fine structure uses synchrotron x-ray radiation to study the absorption of x-rays by an atom at energies near and above the core-level binding energies. It is an element specific technique and, therefore, can be used for the analysis of amorphous and disordered liquid complexes. The position of the absorption edge and the peaks surrounding the edge (near x-ray absorption fine structure) reveal information about oxidation state, covalency (increasing ligand character of metal d-orbitals), and molecular symmetry of the site. For example, higher oxidation state metals have higher positive charge, making it slightly more difficult to photodissociate a 1-s electron. This shifts the K edge to higher energy. Spectral features further from the absorption edge (extended x-ray absorption fine structure) reveal direct, local structural

information about the atomic neighborhood of the element being probed, including the numbers of ligands, the identity of the ligand atoms, and their precise radial distances. The complexes that form at  $\text{TiO}_2$  surfaces in aqueous environments in the presence of surfactants and ions have been studied using x-ray absorption spectroscopy techniques by a variety of researchers (15–18).

---

## 9. References

---

1. Dubrovinsky, L. S.; Dubrovinskaia, N. A.; Swamy, V.; Muscat, J.; Garrison, N. M.; Ahuja, R.; Holm, B.; Johansson, B. The Hardest Known Oxide. *Nature* **2001**, *410*, 653–654.
2. Yanagisawa, K.; Overstone, J. Crystallization of Anatase from Amorphous Titania Using the Hydrothermal Technique: Effects of Starting Material and Temperature. *J. Phys. Chem. B* **1999**, *103*, 7781–7787.
3. Diebold, U. The Surface Science of Titanium Dioxide. *Surface Science Reports* **2003**, *48*, 53–229.
4. Kutty, T. R. N.; Avudaithai, M. *Mat. Res. Bull.* **1988**, *23*, 725–734.
5. Ramamoorthy, M.; Vanderbilt, D.; King-Smith, R. D. First-Principles Calculations of the Energetics of Stoichiometric  $\text{TiO}_2$  Surfaces. *Phys. Rev. B* **1994**, *49*, 16721–16727.
6. Charlton, G.; Howes, P. B.; Nicklin, C. L.; Steadman, P.; Taylor, J. S. G.; Muryn, C. A.; Harte, S. P.; Mercer, J.; McGrath, R.; Norman, D.; Turner, T. S.; Thornton, G. Relaxation of  $\text{TiO}_2(110)$ -(1 x 1) Using Surface X-Ray Diffraction. *Phys. Rev. Lett.* **1997**, *78*, 495–498.
7. LaFemina, J. P. Total Energy Computations of Oxide Surface Reconstructions. *Crit. Rev. Surf. Chem.* **1994**, *3*, 297.
8. Zschack, P.; Cohen, J. B.; Chung, Y. W. Structure of the  $\text{TiO}_2(100)$  1 × 3 Surface Determined by Glancing Angle X-Ray Diffraction and Low Energy Electron Diffraction. *Surface Science* **1992**, *262* (3), 395–408.
9. Henderson, M. The Interaction of Water With Solid Surfaces: Fundamental Aspects Revisited. *Surface Science Reports* **2002**, *46* (1–8), 1–308.
10. Sunagawa, I. *Morphology of Crystals*; Terra Scientific Publishing Co.: Tokyo, Japan, 1987.
11. Stumm, W. Reactivity at the Mineral-Water Interface: Dissolution and Inhibition. *Colloids Surfaces* **1997**, *120*, 143–166.
12. Thiel, P.; Madey, T. The Interaction of Water With Solid Surfaces: Fundamental Aspects. *Surface Science Reports* **1987**, *7*, 211–385.
13. Hayes, K. F.; Leckie, J. O. Modeling Ionic Strength Effects on Cation Adsorption at Hydrous Oxide/Solution Interfaces. *Journal of Colloid Interface Science* **1987**, *115*, 564–572.

14. Brown, G. E. Metal Oxide Surfaces and Their Interactions with Aqueous Solutions and Microbial Organisms. *Chemical Reviews* **1999**, *99* (1), 77–172.
15. Chen, L. X.; Rajh, T.; Jager, W.; Nedeljkovic, J.; Thurnauer, M. C. X-Ray Absorption Reveals the Surface Structure of Titanium Dioxide Nanoparticles. *J. Synchotron Rad.* **1999**, *6*, 445–447.
16. Kriventsov, V.; Kochubey, D.; Tsodikov, M.; Navio, J. XAS Study of the Structured Modified Oxides of Titanium. *Nuclear Instruments and Methods in Physics Research A* **2001**, *470*, 331–335.
17. Manzini, I.; Antonioli, G.; Lottici, P.; Gnappi, G.; Montenero, A. X-Ray Absorption Study of Titanium Coordination in Sol-Gel Derived  $\text{TiO}_2$ . *Physica B* **1995**, *208 and 209*, 607–608.
18. Wasemaker, M.; Lutzenkirchen-Hecht, D.; Keil, P.; van Well, A.; Frahm, R. Quasi-In-Situ Reflection Mode XANES at the Ti K-Edge of Lithium Intercalated  $\text{TiO}_2$  Rutile and Anatase. *Physica B* **2003**, *336*, 118–123.

NO. OF  
COPIES ORGANIZATION

1 DEFENSE TECHNICAL  
(PDF INFORMATION CTR  
ONLY) DTIC OCA  
8725 JOHN J KINGMAN RD  
STE 0944  
FORT BELVOIR VA 22060-6218

1 US ARMY RSRCH DEV &  
ENGRG CMD  
SYSTEMS OF SYSTEMS  
INTEGRATION  
AMSRD SS T  
6000 6TH ST STE 100  
FORT BELVOIR VA 22060-5608

1 DIRECTOR  
US ARMY RESEARCH LAB  
IMNE ALC IMS  
2800 POWDER MILL RD  
ADELPHI MD 20783-1197

3 DIRECTOR  
US ARMY RESEARCH LAB  
AMSRD ARL CI OK TL  
2800 POWDER MILL RD  
ADELPHI MD 20783-1197

ABERDEEN PROVING GROUND

1 DIR USARL  
AMSRD ARL CI OK TP (BLDG 4600)